IBPSA-ENGLAND BSO12

First Building Simulation and Optimization Conference
Loughborough, UK
10-11 September 2012

RELIABILITY OF CO-HEATING MEASUREMENTS

Ir.-arch. Geert Bauwens[1], Dr. Ir.-arch. Piet Standaert[2], Ir. Frédéric Delcuve[3] and Prof. Dr. Ir.-arch. Staf Roels[1]
[1]KU Leuven – Building Physics Section – Department of Civil Engineering, Leuven, Belgium
[2]Physibel, Maldegem, Belgium
[3]Knauf Insulation – Building Science, Mont-St-Guibert, Belgium

ABSTRACT

The energy performance of a building is primarily determined by the thermal performance of the building envelope. Several studies show, however, that the actual 'as-built' performance can differ significantly from the theoretical, calculated value. Characterisation of building performances based on in situ dynamic measurements can help to bridge this gap between 'designed' and 'as-built' performances.

A common method to evaluate the thermal performance of a building in situ is the co-heating test. This test is a quasi-stationary method based on the linear regression analysis of dynamic measurement data. This paper investigates the accuracy of the method for a simple building fabric component.

INTRODUCTION

In order to reduce the energy use of buildings, several countries have put forward more stringent demands on the energy performance of new buildings and renovated buildings. Without exception, these buildings are characterised or awarded a label in the design phase, by calculating the theoretical energy use. Several studies, however, show that the actual 'as-built' performance can differ significantly from the theoretical, calculated value (Bell et al., 2010, Lowe et al., 2007). This difference can among others be attributed to the applied materials that differ from the designated ones, poor detailing and/or workmanship issues and physical phenomena such as thermal bridging, wind washing, air looping, ...

The energy performance of a building is, apart from installed systems and building usage, primarily determined by the thermal characteristics of the building envelope. The thermal performance characterisation of a building, based on dynamic measurement data, is therefore a first step to bridge the gap between the 'designed' and the 'as-built' energy performance of the building.

A typical method to do so is the co-heating test. With a co-heating test the total heat loss coefficient – combined transmission and ventilation heat loss – in W/K and the solar aperture in m^2 of an unoccupied dwelling are estimated. During the test, the dwelling is homogeneously heated to an elevated steady-state interior temperature (e.g. 25°C), using electric heaters. The electrical energy use necessary to retain this elevated temperature, the indoor and outdoor temperatures, wind speed and direction, and solar radiation are monitored throughout the test.

A method similar in approach to the steady-state co-heating test is the primary and secondary terms analysis and renormalisation (PSTAR) test. Here, a short-term heating and cooling-down procedure is adopted to calibrate a thermal audit description model of the building, by renormalizing the considered heat flows based on hourly averaged measurement data and linear regression techniques. Aside from estimating the total heat loss and solar aperture coefficients, the adopted procedures allow the PSTAR test to estimate the effect of the inherent thermal mass of the dwelling (Subbarao, 1988).

This paper, however, solely focuses on the 'pure' co-heating test, which essentially consists of one heating procedure stretched over a longer period of time. The effect of charging and discharging the thermal mass of the building is diminished, by establishing a stationary interior temperature and averaging the measurement data over a sufficient time-span.

The analysis of co-heating measurement data is commonly done using linear regression techniques. The advantage over plain averaging is that possible outliers can be taken into account in a more sensible way. However, to limit possible inaccuracies, the assumptions made during the analysis need to be considered carefully. In this paper, the different practiced quasi-stationary co-heating data analysis methods, based on simple and multiple linear regressions are collected, discussed and applied on daily average measurement data for a simulated cavity wall component. By evaluating the methods based on simulation data, measurement noise sources can be eliminated.

Co-heating methodology

The co-heating test essentially assumes the following heat balance on the investigated building (Everett, 1985):

$$Q + R.S = (\sum A.U + C_v).\Delta T \quad (1)$$

with Q = energy supplied to the building by heaters and dissipated by ventilators [W]; S = global solar radiation measured by local weather station [W/m2]; ΔT = temperature difference inside-outside.
The parameters R [m^2] and (∑A.U + Cv) [W/K] express the relation between Q as a dependent variable and S and ΔT as independent variables. R can be read as a kind of global solar aperture which takes into account the non-perpendicular incidence of solar radiation, geometry (including possible shading) and orientation of the building, solar absorption, solar energy transmittance factor and surface of the glazing in the building envelope.

The parameters of interest are generally determined by applying simple or multiple linear regression techniques on the acquired co-heating measurement data, assuming Eq. 1.

The energy supplied to the interior under the form of electrical energy can – on a daily average basis – be corrected for solar gains and plotted as a function of ΔT. This correction implies that an assumption is made for the solar aperture parameter R. As illustrated in Fig. 1, the slope of the regression line resulting from a simple linear regression on this corrected measurement data set yields an indication of the overall heat loss coefficient (Bell et al., 2010).

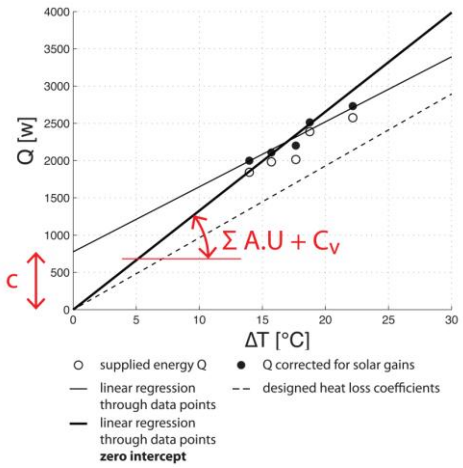

Figure 1 – Illustration of a simple linear regression assuming fictive co-heating measurement data, corrected for solar gains.

An alternative to the method described above is to – aside from ΔT – consider S as an additional independent variable explaining the variability of Q. Multiple regression techniques allow to determine both (∑A.U + C_v) and R in Eq. 1 (Lowe et al., 2007, Everett, 1985)

By dividing all terms in Eq. 1 by ΔT, an equation is attained on which a simple linear regression can be performed, assuming dependent variable Q/ΔT and independent or explanatory variable S/ΔT. An estimate of (∑A.U + C_v) is then given by the intercept (Everett, 1985).
Note that this mathematical transformation implicitly forces the above described multiple linear regression through zero. In both of the earlier mentioned cases, a non-zero intercept is possible due to discrepancies between the measurement data and the assumed stationary model to which it is fitted.

Decoupling of transmission and ventilation heat loss
After applying one of the methods described above, the overall heat loss coefficient can be decoupled into a transmission heat loss and ventilation heat loss, based on an estimate of the air change rate over the course of the measurement period (Bell et al., 2010).

TEST CASE

In this paper, a co-heating test is simulated on a simple cavity wall component, as depicted in Figure 2. Thus, instead of using measured heat loss data on a real building, simulated data on one component are used in this study. This way, as the U-value of the component is known and measurement uncertainty can be avoided, the reliability and 'theoretical' accuracy of the method can be studied.

Although the test case considered is fairly straightforward, it is seen that the fluctuating weather conditions, combined with the thermal inertia of the wall component, introduce transient effects.

Wall properties
Table 1 shows the wall component properties. The theoretical U-value thus becomes:

$$U_{EN} = \frac{1}{\frac{1}{h_e} + Rwall + \frac{1}{h_i}} = 0.27 \text{ W/m}^2\text{K}. \quad (2)$$

This value will be used throughout the paper as a target value to give an indication on the accuracy of the proposed analysis methods and their assumptions, bearing in mind that this value assumes the properties collected in Table 1. The theoretical value assumes e.g. constant surface coefficients on inner and outer surface while the heat exchange at these boundaries is calculated in a more precise manner in the simulations, as shown in Table 2.

	d [mm]	**λ** [W/mK]	**ρc** [kJ/m^3K]	**h** [W/m^2K]	**R** [m^2K/W]
outdoors				25	0.04
brickwork	90	0.9	1554		0.10
insulation	90	0.03	30		3.00
brickwork	140	0.32	882		0.44
gypsum	15	0.43	1200		0.03
indoors				7.7	0.13
total					**3.74**

Table 1 – Insulated cavity wall properties. d = thickness of wall layers, λ = thermal conductivity, ρc = heat capacity; h = total surface heat transfer coefficient, R = thermal resistance.

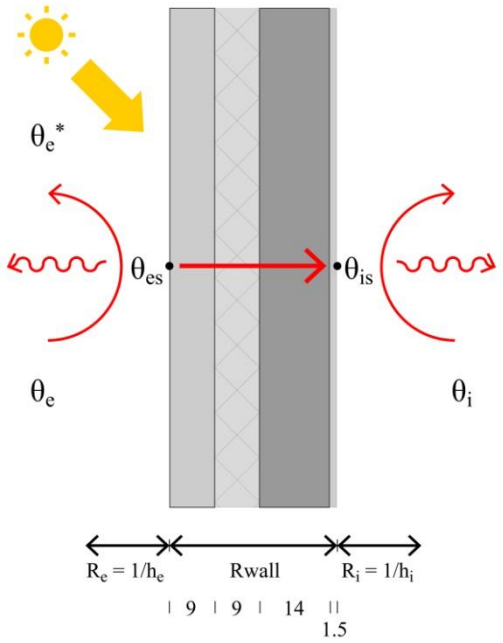

Figure 2– Wall properties and assumed heat transfer mechanisms.

$q_{esc} = h_{ec}(\theta_e - \theta_{es})$	q_{esc}	external surface convective heat flux
	h_{ec}	variable convective heat transfer coefficient = 5.85 $v^{0.52}$
	θ_e	external air temperature
	θ_{es}	external surface temperature
$q_{esr} = \varepsilon\sigma(T_{es}^4 - T_{e,rad}^4)$	q_{esr}	external surface radiative heat flux
	ε	external surface emissivity = 0.9
	σ	Stefan-Boltzmann constant = 5.67 10^{-8} W/m^{2}K^4
	T_{es}	absolute external surface temperature
	$T_{e,rad}$	average radiative temperature environment
solar radiation		solar absorption factor of external surface α_K = 0.75
		south oriented
$q_{isc} = h_{ic}(\theta_i - \theta_{is})$	q_{isc}	internal surface convective heat flux
	h_{ic}	variable convective heat transfer coefficient = 1.46 $(\theta_i - \theta_{is})^{1/3}$
	θ_i	internal air temperature
	θ_{is}	internal surface temperature
$q_{isr} = \varepsilon\sigma(T_{is}^4 - T_{i,rad}^4)$	q_{isr}	internal surface radiative heat flux
	ε	internal surface emissivity = 0.9
	σ	Stefan-Boltzmann constant = 5.67 10^{-8} W/m^{2}K^4
	T_{is}	absolute internal surface temperature
	$T_{i,rad}$	average radiative temperature interior room = 20 + 273.15 K

Table 2 – Heat exchange with indoor and outdoor environment as incorporated in the simulations.

Simulation assumptions

A south-oriented wall component with an area of 1 m^2 is simulated over a whole year, assuming climate data of Ukkel, Belgium. The thermal conductivity, density and specific heat of all materials are taken constant. A constant indoor air temperature of 20°C is maintained. Inside and outside surface heat fluxes are decoupled in a convective and radiative heat transfer component (Table 2). The combined heat flux [W/m^2] at the interior side of the cavity wall as a function of time is continuously recorded in the simulation. This heat flux is considered as an estimate of the electric energy Q needed to sustain the elevated indoor air temperature.

The subject of this study is limited to transmission heat losses. The wall is assumed airtight and ventilation heat losses have hence not been considered. The heat balance can therefore be simplified to (C_v = 0 and A = 1m^2):

$$Q + R.S = U.\Delta T \quad (3)$$

Throughout this paper, daily averages of both the dependent variable Q and independent variables S and ΔT are considered.

It is important to note that $Q = q_{isc} + q_{isr}$ is allowed to become negative in the simulations. As the indoor temperature is kept at 20°C in the simulations, this actually corresponds to cooling in summer conditions, whereas in reality the indoor air temperature will rise above the intended value.

STATIONARY ANALYSIS OF AN INSULATED CAVITY WALL

In this paper, the accuracy of the quasi-stationary analysis of co-heating measurement data, based on linear regression techniques, will be investigated on the simulated measurement data. All of the considered methods take Eq. 3 as a basis. The influence of taking the thermal inertia of the test case component into account and forcing the intercept of the linear regression line or surface through the origin is investigated for all considered methods.

In a first section, a simple linear regression will be assumed by solely looking at ΔT as an independent variable.
In the second section, S is added as an additional independent variable explaining the variability of Q. A multiple linear regression can thus be performed. By performing a transformation on Eq. 3, the independent variable becomes Q/ΔT and the independent or explanatory variable becomes S/ΔT.
The third section looks at the simple linear regression on this transformed equation.

In a last section, possible improvements to Eq. 3 are suggested to better correct for thermal lag effects and to include more physical information in the model.

In the cases studied where solar radiation as an explanatory variable is considered, the horizontal global solar radiation was converted to the global solar radiation perpendicular to the south-oriented vertical wall plane.

Throughout this section, the accuracy of the presented analysis methods is visualised as a scattered collection of U-values resulting from the specified regression analysis on data acquired during simulated measurement campaigns with different starting dates and durations. In order to obtain a sufficient number of data points, the minimum duration has been set to 2 days in the case of the methods discussed in the first sections, and to 3 days for the extended model introduced in the last section.

Simple linear regression with ΔT as an independent variable

In this case, only ΔT is considered as an independent variable, explaining the variability of the supplied energy Q.

$$Q = U.\Delta T + c \quad (4)$$

Figure 3 (top) shows the U-values found by applying simple linear regression on measurement data acquired during different measurement campaigns with different durations over the course of one year. In the case of short measurement campaigns, a very large spread in calculated U-values is seen. Measurement campaigns in summer, associated with a smaller average Q (blue coloured dots on the graph), show an even larger spread which persists until around 50 measurement days, after which it can be seen to influence longer lasting campaigns, since these are likely to include a period of summer days. Eventually the analysis results of longer measurement campaigns converge towards an overestimate of the U-value.

Thermal lag

From a harmonic analysis, it can be derived that there is an important phase shift (10h15 for a 24h period signal) between the internal flux, or the energy that needs to be supplied, and the external temperature. Due to this phase shift, ΔT at time t will not be representative for the needed energy supply at that time. To cope with this thermal lag induced by the thermal inertia of the cavity wall, the supplied energy at time t can be correlated with an average of ΔT at time t and t-1.

$$Q_t = U.\left(\frac{\Delta T_t}{2} + \frac{\Delta T_{t-1}}{2}\right) + c \quad (5)$$

Essentially, a correlation is made with a ΔT-value representative for the current time step and a time step in history. The positive effect on the U-value estimation is visualized in Figure 3 (middle).

Zero intercept (c = 0)

In summer periods (low average Q), regularly accompanied with high solar radiation, the linear regression lines are likely to show negative intercepts (c < 0). Rotating these lines towards a zero intercept is naturally accompanied by a decrease of slope, which explains the stratified behaviour in Figure 3 (bottom).

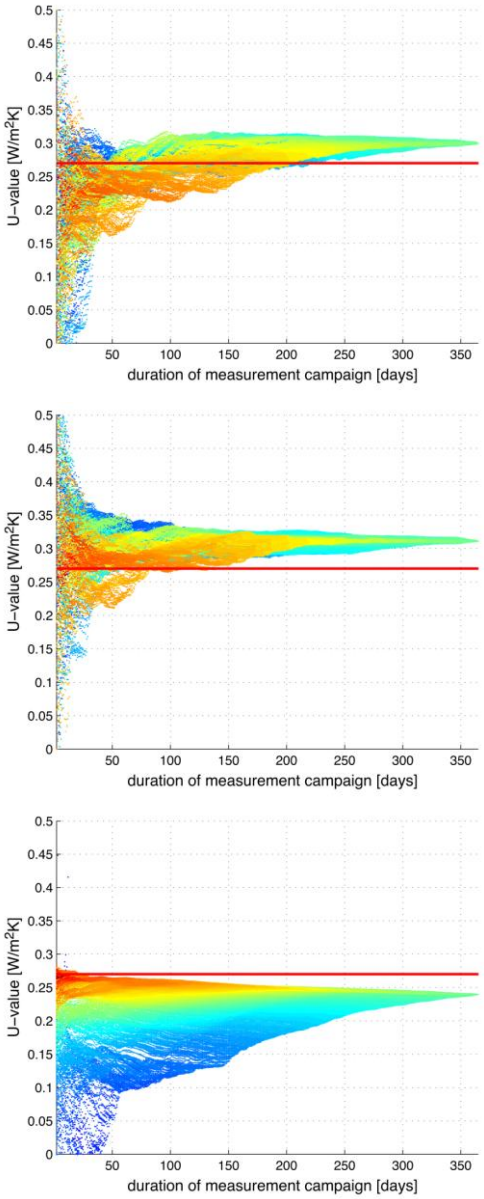

Figure 3 – U-value estimation through simple linear regressions applied on measurement campaign data with different starting dates and duration based on simulations over the course of one year. Top: basic regression; middle: thermal lag taken into account; bottom: thermal lag taken into account and intercept forced through zero (c = 0). The data points are coloured according to the average Q over the course of the measurement campaign: red points indicate a high average Q, blue points indicate a low average Q.

Multiple linear regression with ΔT and S as independent variables

In this section, the solar radiation is introduced as an explanatory variable. Together with ΔT, more of the variability of the supplied energy will be explained.

$$Q = U.\Delta T - R.S + c \quad (6)$$

Figure 4 depicts the results of applying multiple regression on the acquired simulated measurement data, assuming Eq. 6.

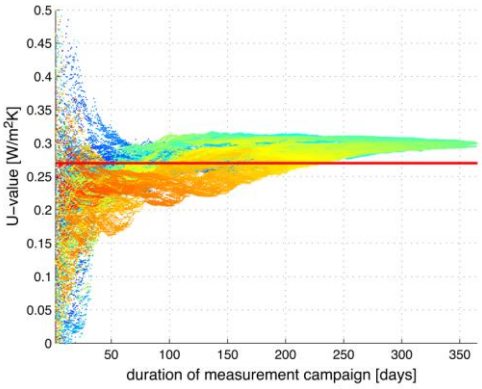

Figure 4 – U-value estimation through multiple regressions applied on measurement campaign data with different starting dates and duration based on simulations over the course of one year. The data points are coloured according to the average Q over the course of the measurement campaign: red points indicate a high average Q, blue points indicate a low average Q.

The result is similar to Figure 3. This is likely explained by the fact that the influence of S can be expected to be limited, since a wall component without any glazed opening is studied.

In summer, days with low Q and low ΔT are common. These data points can corrupt the result of the regression, by the combined effect of:

- transient effects that become more important,
- cantilever effect of points at the outskirts of the scatter (low Q and low ΔT).

When solely looking at measurement campaigns in the cold winter months (October-March), thereby excluding measurement campaigns that begin in or continue into the warmer half of the year (April-September), it is seen that the scatter plots show a much better convergence to the target U-value (Figure 5).

Thermal lag

Figure 5 (middle) clearly shows that taking the history on S and ΔT into account, yields a considerable improvement in accuracy and a decrease of the necessary duration of measurement campaigns to attain the target U-value.

Zero intercept

Comparing the bottom and middle plot in Figure 5, it can be seen that the assumption of a zero intercept greatly increases the accuracy of the regression analysis. The U-value now converges to a U-value estimation slightly larger than the target U_{EN}-value of 0.27. This difference can most likely be attributed to a possible overestimation of h_e in the target value.

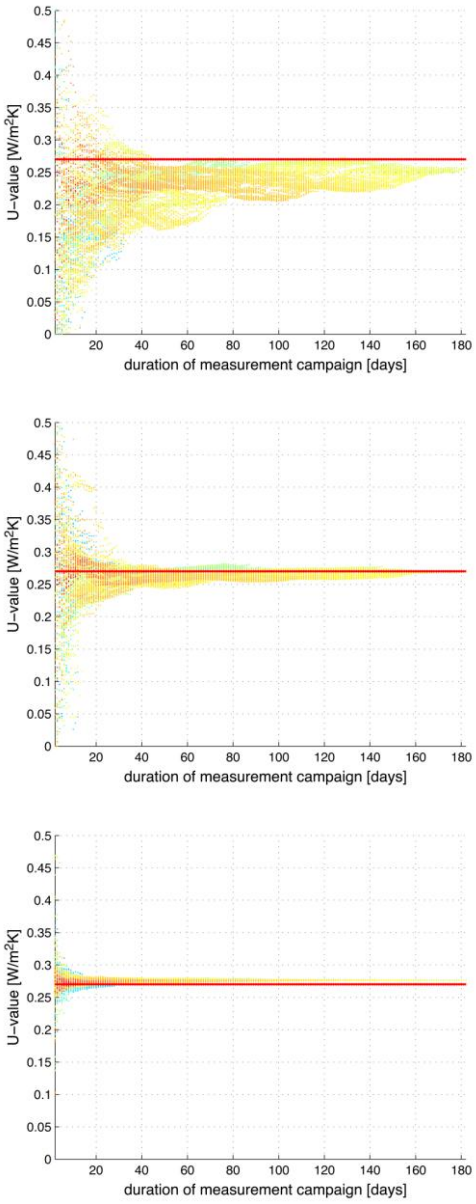

Figure 5 - U-value estimation through multiple regressions applied on measurement campaign data with different starting dates and duration, but limited to the winter season. Top: basic regression; middle: thermal lag (ΔT and S) taken into account; bottom: thermal lag (ΔT and S) taken into account and intercept forced through zero (c = 0). Again, the data points are coloured according to the average Q over the course of the measurement campaign: red points indicate a high average Q, blue points indicate a low average Q.

Simple linear regression on transformed equation

The multiple linear regression discussed in the previous section can be mathematically transformed to a simple linear regression, by dividing all terms in Eq. 6 by ΔT:

$$Q/\Delta T = U - R.S/\Delta T \quad (7)$$

The U-value estimation then is found as the intercept of the simple linear regression line with the y-axis. As stated above, this mathematical transformation implicitly forces the above described multiple linear regression through zero (c = 0).

Figure 6 (bottom) shows a good U-value estimation when ΔT and S are taken into account, including the assumption of the wall phase shift (Eq. 5) on both signals.

When only considering winter period measurements, the result is virtually the same as the bottom plot in Figure 5, illustrating the similarity with the multiple linear regression with zero intercept, as described above.

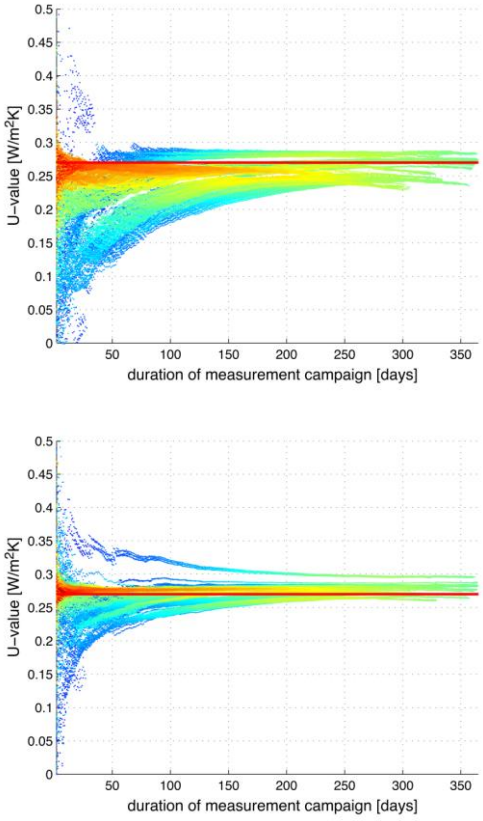

Figure 6 – U-value estimation through linear regressions assuming a transformed equation applied on measurement campaign data with different starting dates and duration based on simulations over the course of one year. Top: basic regression; bottom: thermal lag (ΔT and S) taken into account. The data points are coloured according to the average Q over the course of the measurement campaign: red points indicate a high average Q, blue points indicate a low average Q.

In the case of measurement data completely or partly acquired during summer, however, the results of this analysis method are easily corrupted due to ΔT fluctuating around zero. As can be seen in Figure 7, this scales the according Q/ΔT and S/ΔT values dramatically, resulting in rapidly fluctuating positive and negative values.

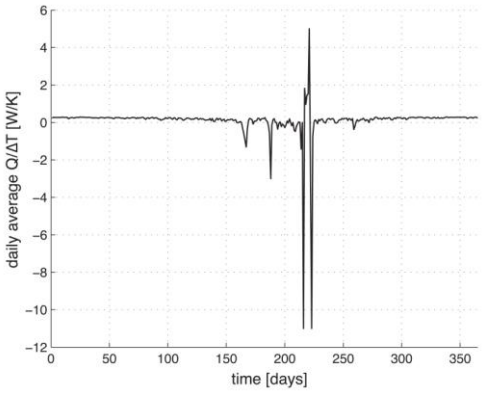

Figure 7 – Variation of Q/ΔT over the course of one year. Note the important fluctuations during the summer period (day 91 to 273).

This phenomenon is clearly illustrated by the irregular behaviour of the blue to green data points in Figure 6. Additionally, it can be seen that there are multiple U-value estimates to which seems to be converged, due to the influence of such anomalies occurring during the measurement campaign. Evidently, when considering measurement campaigns stretching over a whole year, the U-value estimates are equal regardless of the starting date.

Possible improvements to the regressions

The regression models presented above can be extended in order to:

- explain more of the variability of Q,
- quantify the thermal lag;
- include more physical information.

Correction for thermal lags

Above, correlations were assumed with ΔT and S averaged over time t and t-1, to improve the U-value estimations. In essence, this assumes a phase shift of half a day. In reality, the phase shift of the walls and other building components will often be unknown. To avoid this assumption and to further improve the correlation, ΔT and S can be written as a weighted average of their respective values at time t and t-1, where the weight factors are fitted to the measurement data as part of a multiple linear regression of the form:

$$Q = U.(\alpha_1\Delta T_t + \alpha_2\Delta T_{t-1}) - R.(\beta_1 S_t + \beta_2 S_{t-1}) + c \quad (8)$$

assuming $\alpha_1 + \alpha_2 = 1$ and $\beta_1 + \beta_2 = 1$.

Figure 8 shows the U-value and thermal lag estimates resulting from applying Eq. 8 on the measurement data acquired during winter.

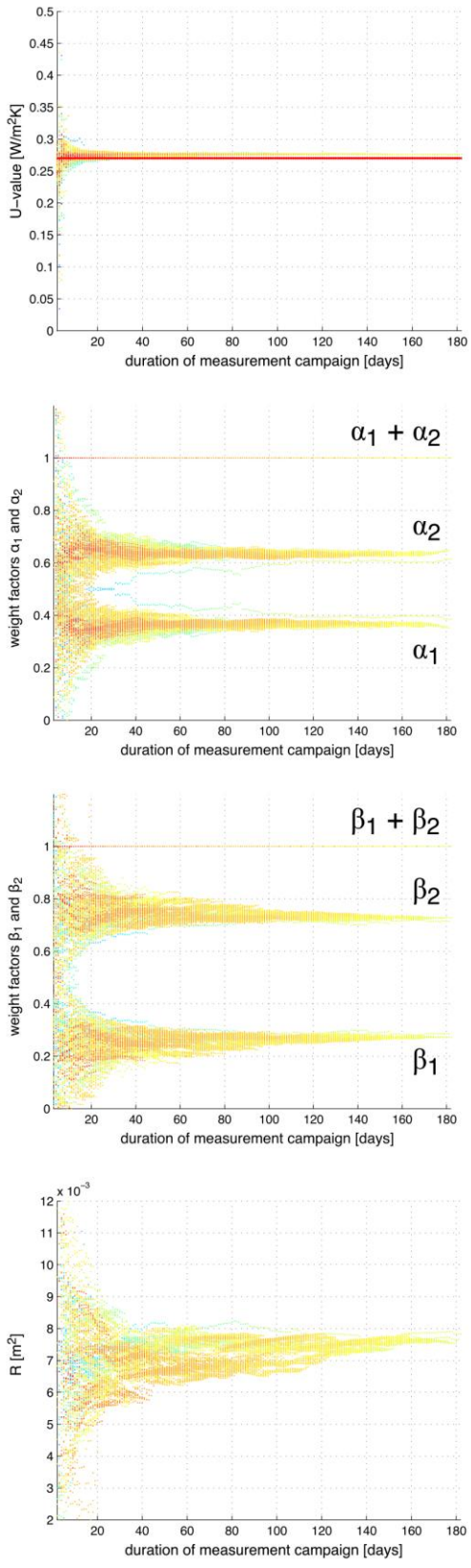

Figure 8 – Multiple regressions applied on measurement campaign data with different starting dates and duration, but limited to winter season, thereby assuming Eq. 8. Thermal lag (ΔT and S) taken into account and intercept forced through zero (c=0). Top: U-value estimation; upper middle: estimates of α_1 and α_2; lower middle: estimates of β_1 and β_2; estimate solar aperture coefficient R. The data points are again coloured according to the average Q over the course of the measurement campaign.

The middle plots in Figure 8 show that the thermal lag assumption made in Eq. 5 is likely to be a slight underestimation of the thermal inertia of the insulated cavity wall ($\alpha_1 < \alpha_2$ and $\beta_1 < \beta_2$). Note, however, that the determination of the weight factors is associated with a considerable error, especially in measurement campaigns no longer than 3 weeks.

Back to the physics: including more information in the model

Essentially, Q is dependent on the outside surface temperature θ_{es}, the inside reference temperature θ_{rs} and the wall characteristics:

$$Q = \frac{(\theta_{es} - \theta_{rs})}{R_{wall} + \frac{1}{h_i}} \quad (9)$$

with θ_{es} dependent on the outside air temperature θ_e, the vertical global solar radiation S and the outside heat transfer coefficient h_e. Using the equivalent outside temperature θ_e^*, Q can be written to express these dependencies (neglecting the influence of long-wave radiation):

$$Q = U.(\theta_{rs} - \theta_e^*) = U.\Delta T - \frac{U.\alpha_K}{h_e}.S \quad (10)$$

$\theta_{rs} = (\theta_i + \theta_{ri})/2 \approx \theta_i$

θ_{rs}	reference temperature inside,
θ_i	indoor air temperature,
θ_{ri}	average radiation temperature of walls surrounding interior space.

$$\theta_e^* = \theta_e + \frac{\alpha_K.S}{h_e} \quad (11)$$

θ_e	outside air temperature,
α_K	surface absorption,
S	vertical global solar radiation,
h_e	average radiation temperature of walls surrounding interior space.

Eq. 10 essentially describes the same phenomenon as was described in Eq. 6, only it includes more physical information.

Improved model

The suggested improvements can be combined:

$$Q = U.(\alpha_1\Delta T_t + \alpha_2\Delta T_{t-1}) - \frac{U.\alpha_K}{h_e}.(\beta_1 S_t + \beta_2 S_{t-1}) + c \quad (11)$$

As shown in Figure 8, applying multiple regression on this improved model gives us an estimate of U and $R = \frac{U.\alpha_K}{h_e}$, as well as information about the phase shift (α_1, α_2, β_1 and β_2) introduced by the cavity wall. R can be seen to converge towards a value slightly under the calculated target value of 0.0081 m2.

Note that a considerable error is associated with the estimate of R, especially in shorter measurement campaigns. Additionally, an estimate of $\frac{\alpha_K}{h_e}$ can be calculated as R/U. This estimate converges to a value slightly under the calculated target value (α_K = 0.75 and h_e = 25 W/m^{2}K).

DISCUSSION

The present study investigated the reliability of co-heating tests by analysing simulated data on a simple wall component neglecting heat loss due to ventilation.

For the case studied, it has been shown that a fairly good thermal characterisation can be achieved with a limited co-heating measurement campaign duration of 2 weeks, when applying multiple linear regression assuming: ΔT and S as independent variables, a phase shift imposed on ΔT and S, a zero intercept and a sufficiently high average Q. The assumption about the phase shift made in Eq. 5 and the improvement suggested Eq. 8 both yield good results. Restricting the measurements to the winter months increases the probability of attaining measurement campaigns with a sufficiently high average Q, since in winter there is a higher occurrence of days with high ΔT and low S.

It is recommended to determine the solar aperture coefficient R by applying multiple regression, as it allows accounting for opaque surfaces. Additionally, it allows to determine R by data analysis instead of calculation. Important to note, though, is that a large error can be associated with its estimate, in the case of very small R values.

Although good results have been attained, the applied linear regression analysis methods have some restrictions. By assuming Q as a dependent variable and ΔT and S as independent variables, it is implicitly assumed that only Q is associated with a measurement error and no measurement errors are associated with ΔT and S. All realistic measurement data, however, inevitably have errors attached to it.

It is important to note that the weight factor conditions $\alpha_1 + \alpha_2 = 1$ and $\beta_1 + \beta_2 = 1$ do not improve the fit to Eq. 8, since these weight factors do not occur as such in the coefficients resulting from the regression, thus adding no additional information. Similarly, the suggested improvement in Eq. 10 does not improve the regression fit. It does, however, allow to extract more physical information from the same regression analysis.

Not taken into account in this study, an important limitation of the linear regression analysis is that it is unable to distinguish between the constituting building envelope components of a whole building. The method solely determines the total heat loss coefficient $\sum A.U + C_v$. In reality, however, multiple components exist with different heat loss coefficients, different orientations and different thermal capacities. Additionally, the real solicitation of the building envelope is not harmonic and the periodicity of the different weather condition components and their transient effects on the building can differ significantly.

In any case, the use of daily averaged data limits the amount of data points that one can acquire in a certain measurement campaign, and thus limits the complexity of the model that can be fitted applying regression methods. In order to more accurately characterise the thermal performance of a building envelope using co-heating measurement data, it might be advisable to go towards an intrinsically dynamic model, where detailed characteristics of the building envelope components can be determined in a distinguishable way and shorter time intervals allow for more descriptive data points.
A possible solution is system identification, in which the thermal characterisation of the building is achieved by translating it into a physical model and fitting this model to the available dynamic measurement data. System identification therefore offers a sensible way of analyzing co-heating measurement data that are intrinsically dynamic. The physical model comprises a certain configuration of thermal resistances and capacities, tailored to the investigated building and of a complexity that is adapted to the problem at hand. The parameters that govern the exact workings of the model can then be determined by system identification.

ACKNOWLEDGEMENT

The authors wish to thank Knauf Insulation, for setting up an expert network concerned with investigating the gap between the ‘designed’ and ‘as-built’ thermal performances of building envelopes.

REFERENCES

Bell, M., Wingfield, J. & Miles-Shenton, D. 2010. Low carbon housing. Lessons from Elm Tree Mews, Joseph Rowntree Foundation

Everett, R. 1985. Rapid thermal calibration of houses, ERG, Open University Energy Research Group, Milton Keynes UK.

Lowe, R.J. et al. 2007. Evidence for heat losses via party wall cavities in masonry construction. Building Service Engineers Research and Technology, 28 (2), pp. 161-181.

Software used for simulations: Physibel software VOLTRA version 7.0w (2011)

Subbarao, K., 1988. PSTAR – Primary and Secondary Terms Analysis and Renormalization: A Unified Approach to Building Energy Simulations and Short Term Monitoring – A Summary, SERI/TR-254-3347, Golden, CO: Solar Energy Research Institute.